Nuclear surface localization of preequilibrium reactions at low energies

M. Avrigeanu, A. Harangozo, and V. Avrigeanu
Institute of Physics and Nuclear Engineering, P.O. Box MG-6, 76900 Bucharest, Romania

A. N. Antonov
Institute of Nuclear Research and Nuclear Energy, Sofia 1784, Bulgaria
(Received 30 May 1996)

Average quantities related to the characteristics of the nucleon-nucleon (NN) interaction along the trajectory of the projectile in preequilibrium reactions are calculated by using the semiclassical method to follow the incoming particle's path in the nuclear target. The radial dependences of the nucleon's mean free path and the probability for the first NN collision have pointed out the surface character of the first NN interaction in multistep reactions even at low energies. In the local density approximation an average Fermi energy and an average strength of the effective NN interaction V_0 along the trajectory of the incident nucleon are obtained with respect to both the nuclear density and the first NN-collision probability. Good agreement is found between the average strengths obtained with the Hartree-Fock potential plus the dispersive component and by using the parametrization based on the Brueckner-Hartree-Fock nuclear matter calculations. It is also shown that the nuclear-density dependence of the effective NN interaction may account for the low-energy phenomenological V_0 values which are much more increased in comparison with any prediction. [S0556-2813(96)05411-8]

PACS number(s): 24.60.Gv, 21.30.Fe, 24.10.−i

I. INTRODUCTION

The preequilibrium nuclear reactions which link the extreme mechanisms of the compound nucleus and the direct reactions have been studied for some decades. Various semiclassical models and quantum-statistical theories (e.g., [1]) describe them as passing through a series of particle-hole excitations caused by nucleon-nucleon (NN) interactions. Usually a simple Yukawa force of 1 fm range has been used in calculations and thus the effective NN-interaction strength V_0 is the only free parameter of the multistep direct (MSD) and multistep compound (MSC) reaction theory of Feshbach, Kerman, and Koonin (FKK) [2]. It should be noted, however, that even when a consistent standard parameter set has been used and several other effects have been taken into account [3,4] some discrepancies in the systematics of the phenomenological V_0 values used in FKK-MSD calculations still exist. It was suggested, e.g., that a more realistic NN interaction has to be involved [4,5], while it is already proved [6] that the so-called M3Y interaction may perhaps not be as good as assumed.

The possibility to include in the model some effects which have been neglected until now [7] is presently taken into account in relation with the particle-hole state densities. It is especially the case of the less exact but global semiclassical state densities, assumed not to be so crucial in the past, while errors in them could be compensated by rescaling of the effective NN-interaction strength [6]. Actually, combinatorial calculations of the partial state density (PSD) performed in the space of realistic shell-model single-particle levels have already been used in MSC calculations by Herman *et al.* [8] or developed in this respect [9,10]. PSD's calculated by a shell model are involved in MSD studies as well [8]. However, the strong dependence of the microscopic PSD on the basic set of single-particle levels is the main among the several shortcomings inherent in the method (e.g., [11,12]), which may explain the general use of the semiclassical Williams-type [13] formulas even at present within a quantum formalism.

On the other hand, it is well known that the direct reaction amplitude is dominated by contributions from the nuclear surface region due to the radial localization of the important partial waves, and also by considering (for short wavelengths) the flux patterns associated with the ingoing and outgoing distorted waves [14]. That is why Watanabe *et al.* [3] have estimated the incident local energies at the radius $R=1.25A^{1/3}$, where A is the mass number, in the analysis of the V_0 values extracted from both (n,n') and (p,p') scattering at 12–26 MeV, thus paying attention to the difference in the charge and isospin of the projectile. Since the first step of the preequilibrium processes is essentially an extension of direct reactions in the continuum, a limited energy of the possible hole excitation due to the shallower nuclear potential within the nuclear surface was assumed for this step even in semiclassical models [15–17]. The dependence of the effective NN-interaction strength on the realistic density of finite nuclei was involved too [18] in order to obtain consistent MSD and MSC results. Nevertheless, it is now considered that the surface effects should be taken into account not only through the change of the density around the nuclear surface [19].

Actually, it has been shown within the semiclassical distorted wave (SCDW) model [20–22] that the NN collision in the nucleus may be considered as localized when the final nuclear states lie in the continuum of the excitation spectrum as is usually the case of preequilibrium reactions. Kawai *et al.* have thus calculated the probability of the incident particle to reach the point $\mathbf{r}$ where the first NN collision occurs, and its propagation (with a loss of the flux by absorption) to a point where the second collision takes place and the out-

going particle escapes. The SCDW model is based on the distorted-wave Born approximation (DWBA) expansion, greatly simplified by using the local semiclassical approximation to the distorted waves, the eikonal approximation to the intermediate state Green functions, and the assumption of the local density Fermi-gas model for the nuclear states. While the geometrical optics approximation to the distorted waves was used initially [20], even the semiclassical approximation of the respective quantal wave functions makes it possible to take into account contributions from the regions which are inaccessible to classical trajectories.

In this paper we study the surface localization of the first *NN* collision in preequilibrium reactions at low energies by using the semiclassical method to follow the incoming particle's path within the nuclear target. The first preequilibrium stage has a particular significance at these energies for which the two-step scattering in MSD processes is negligibly small [23]. It has got a specific description also within the semiclassical models mentioned above. However, the use of a constant reduced potential depth [16] or the local incident energy calculated just at the nuclear radius R [3] could be difficult to justify. Because of that we look for a radial dependence of the first two-body collision probability in order to use it for calculations of various average quantities related to preequilibrium reactions.

In Sec. II we calculate the local mean free path $\lambda(r)$ given by the optical-model potential and present briefly the main points of the approximate derivation of the expression for the related first *NN*-collision probability. The average Fermi energy for the first *NN* interactions in preequilibrium reactions is analyzed in Sec. III. Within the same frame we discuss in Sec. IV the systematics of the phenomenological V_0 values used in FKK-MSD calculations and present the calculated average strength of the effective *NN* interaction $\underline{V}_0$ along the trajectory of the incident nucleon for the first *NN* collision. The conclusions from the work are given in the final Sec. V.

II. FIRST *NN*-COLLISION PROBABILITY

The probability of the first interaction between the projectile and one of the target nucleons to occur in the diffuse nuclear surface is often considered by using the mean free path (MFP) λ of the incident particle in nuclear matter. In this case the phenomenological nucleon λ values [24] which are large compared with the nuclear size better support the assumption that the reaction takes place in the nuclear volume. The microscopic models which use the energy-momentum dispersion relations in the case of nucleons in nuclear matter have provided larger values of the MFP too (especially at energies lower than e.g. 50 MeV) when the final-state Pauli blocking [25] and the nonlocality of the nuclear optical potential are taken into account [26–28]. We should note, however, that first, even the phenomenological central MFP $\lambda(r=0)$ is ambiguous and depends on the parametrization chosen for the radial shape of the optical model potential (OMP), smaller values being yet possible [28,29]. Second, it has been shown [30] that only a local MFP $\lambda(r)$ should be considered for finite nuclei and its values can differ enormously from the value in the central region of the nucleus. Alternative quantities like the absorption probability have been considered to be more meaningful.

Nevertheless, it was shown semiclassically [20] that the localization of the first two-body collision in a nuclear reaction leading to the continuum of the residual nucleus is a consequence of the averaging procedure over the final nuclear states. Actually, the outgoing particle is quantum mechanically described by a wave function which is a superposition of emitted waves generated at different points of the nucleus, and so it is generally meaningless to talk about a particular point at which the reaction takes place. However, Kawai proved [20] that the scattered waves arising from different points of the nucleus are incoherent to each other in the higher excitation processes. This is the meaning of the *NN*-collision localization which is thus assumed when the semiclassical approach is expected to be quantitatively reliable, i.e., when the incident and outgoing particle trajectories as well as the momentum of the particle at each point of the trajectory can be considered.

It is known that the semiclassical approximation is applicable when the wavelength of the incident particle fulfills the condition $\lambda\!\!\!^{-} \ll R$ and when the incident energy E_i is much larger than the depth of the respective potential. However, the results obtained by using this high-energy approximation are qualitatively correct even below, e.g., $E_i=100$ MeV [31,32]. The SCDW model has been applied successfully for 62 MeV proton-induced reactions [21,22]. This result seems to be due to the correctness of the assumption that the distorting potential and the density of the nucleus are slowly varying radial functions in comparison with the rapid oscillation of the distorted waves at intermediate and even lower energies. Moreover, we should note the early comparison of the quantal and classical flux of neutrons in a complex optical potential for incident energies from 5 to 30 MeV [33] which showed that the behavior of both the local average flux and its divergence (giving the probability of a collision to occur at a point) can be described quite well at the *higher* limit of this energy range by the geometrical-optics approximation. Large differences have been found in the regions of space where the flux and divergence are small, as in those which are inaccessible by classical trajectories. This drawback has been removed within the SCDW model when the geometrical-optics approximation to the distorted waves [20] was replaced by the use of quantal wave functions [21]. A similar step was made from the pragmatic classical approach [31] to the DWBA analysis of the importance of the first *NN* collision in preequilibrium emission [34]. Therefore, our analysis based on semiclassical techniques should take additional care for nucleon energies lower than, e.g., 20 MeV and consider the results within the respective limits.

The probability of the incident particle to reach the point $\mathbf{r}$ is obtained by means of the strict eikonal approximation [35]. Hence the high-energy approximation to the distorted wave in the incident channel with the wave number $k_i=(2\mu E_i)^{1/2}/\hbar$,

$$\chi_i^{(+)}(\mathbf{r}) \sim \exp\left\{ i\left[\mathbf{k}_i\cdot\mathbf{r} + \int^{\mathbf{r}} d\mathbf{s}\cdot\mathbf{k}_i(\mathbf{s}) \right] \right\}, \tag{1}$$

involves the path of integration along the classical-particle curved trajectory that passes through a given point with the direction of the local wave number vector $\mathbf{k}_i(\mathbf{s})$ given by the

tangent to the path. The complex incident momentum $\hbar\mathbf{k}_i(\mathbf{r})$ inside the target nucleus and the local kinetic energy $E_i(\mathbf{r})=\hbar^2k_i^2(\mathbf{r})/2\mu$ are connected within the local energy approximation

$$E_i(\mathbf{r})+U_{i,\mathrm{eff}}(\mathbf{r})=E_i\,, \tag{2}$$

with the effective potential energy [20] evaluated for the complex distorting potential $V(r)+iW(r)$:

$$U_{i,\mathrm{eff}}(r)=\frac{1}{2}\left\{\frac{\hbar^2k_i^2}{2\mu}+V(r)-\left[\left(\frac{\hbar^2k_i^2}{2\mu}-V(r)\right)^2+W^2(r)\right]^{1/2}\right\}, \tag{3}$$

where μ is the reduced mass. Here we should like to mention that Eq. (2) is the Hamilton-Jacobi equation for the classical action function $S(\mathbf{r})$ which is related to the local momentum by $\mathbf{k}_i(\mathbf{r})=\nabla S(\mathbf{r})$. Therefore, the probability of the incident particle to reach the point $\mathbf{r}$ within an absorbing potential (i.e., with a negative imaginary part) is [20]

$$\frac{k_i(\mathbf{r})}{k_i}|\chi_i^{(+)}(\mathbf{r})|^2\sim\frac{k_i(\mathbf{r})}{k_i}\exp\left[-\int^{\mathbf{r}}ds/\lambda(s)\right]=\frac{k_i(\mathbf{r})}{k_i}\times\exp\left\{-\int_r^{\infty}\frac{dr'}{\lambda(r')}\left[1-\frac{l(l+1)}{k_i^2(r')r'^2}\right]^{-1/2}\right\}, \tag{4}$$

where the attenuation of the advancing distorted wave is given by the inverse of the local MFP of the incident particle:

$$\lambda(r)=\{2\,\mathrm{Im}[k_i(r)]\}^{-1}=\frac{\hbar}{2\mu^{1/2}}\left\{V(r)-\frac{\hbar^2k_i^2}{2\mu}+\left[\left(\frac{\hbar^2k_i^2}{2\mu}-V(r)\right)^2+W^2(r)\right]^{1/2}\right\}^{-1/2}. \tag{5}$$

In the case when $W(r)\ll E_i-V(r)$ the MFP reduces to the usual form (e.g., [1])

$$\lambda(r)=-\frac{\hbar}{(2\mu)^{1/2}}\frac{1}{W(r)}\left[\frac{\hbar^2k_i^2}{2\mu}-V(r)\right]^{1/2}. \tag{6}$$

Next, we are interested in the absorption probability of the ingoing particle along the classical trajectory between the points $\mathbf{r}$ and $\mathbf{r}'$, for the small $|\mathbf{r}'-\mathbf{r}|$. The probability for a collision in a volume V which contains the segment of the classical trajectory between the two points is related to the volume integral of the divergence of the particle flux $\mathbf{J}_i(\mathbf{r})=(\hbar/\mu)|\chi_i^{(+)}(\mathbf{r})|^2\mathbf{k}_i(\mathbf{r})$. Using the curve-linear coordinate system introduced by Kawai [20] it can be shown that this integral becomes approximately

$$-\int_V d\mathbf{r}''\mathrm{div}\mathbf{J}_i(\mathbf{r}'')\sim J_i(\mathbf{r})-J_i(\mathbf{r}'). \tag{7}$$

Dividing the result by the flux at the point $\mathbf{r}$ and accounting for the probability (4), we can write the probability of the first NN collision to occur within a small ds interval along the curved trajectory in the form

$$\frac{k_i(r)}{k_i}\exp\left[-\int^r ds/\lambda(s)\right]\left[1-\frac{J_i(r')}{J_i(r)}\right]. \tag{8}$$

Finally, since

$$|\chi_i^{(+)}(\mathbf{r}')|^2=|\chi_i^{(+)}(\mathbf{r})|^2\exp\left[-\int_{\mathbf{r}}^{\mathbf{r}'}ds/\lambda(s)\right], \tag{9}$$

it becomes, after the averaging over the partial waves too,

$$P(r)=C\sum_l(2l+1)\frac{k_i(r)}{k_i}\exp\left[-\int^{\mathbf{r}}ds/\lambda(s)\right]\times\left\{1-\frac{k_i(r')}{k_i(r)}\exp\left[-\int_{\mathbf{r}}^{\mathbf{r}'}ds/\lambda(s)\right]\right\}, \tag{10}$$

where the normalization constant C is determined by the condition

$$\int_0^{\infty}dr\,P(r)=1, \tag{11}$$

which is related to our interest in the distribution of this probability along the nuclear radius. Equation (10) clearly shows the dependence of the first NN-collision probability on the MFP $\lambda(r)$ which is determined by the imaginary and real parts of the distorting potential. In the case of the central collisions it reduces to the form discussed previously [36].

The general trend of the results given by this formulation is illustrated for neutrons incident on ^{93}Nb at various energies from 10 to 50 MeV (Fig. 1). The global parameter set of the optical potential given by Walter and Guss [37] has been used in this respect. The same potential was also involved to study [3] the systematic behaviour of the strength V_0 and the sensitivity of the respective FKK calculations to the OMP parameters.

The energy and radial dependences of the phenomenological imaginary potential [Fig. 1(a)] are responsible for the corresponding behavior of the local MFP [Fig. 1(b)]. The surface peaking of the imaginary potential at lower energies results in a minimum of $\lambda(r)$ in the region of the nuclear surface. The central imaginary potential depth is small at the lowest energies due to the Pauli-blocking effect and thus $\lambda(0)$ is higher. On the other hand, $\lambda(r)$ is increasing quickly while the nuclear density and consequently the potential well are vanishing. The surface part of the imaginary OMP decreases with the increase of the energy, so that the radial dependence of λ diminishes gradually. At medium energies where the imaginary potential has only a volume component, the MFP values become constant and equal to $\lambda(0)$. The microscopic calculations of the nucleon MFP in finite nuclei using the Thomas-Fermi theory for multiparticle-multihole configurations [38] describe well these trends. It has been thus shown that the interplay between the smaller imaginary potential depth and the smaller local momenta at the nuclear

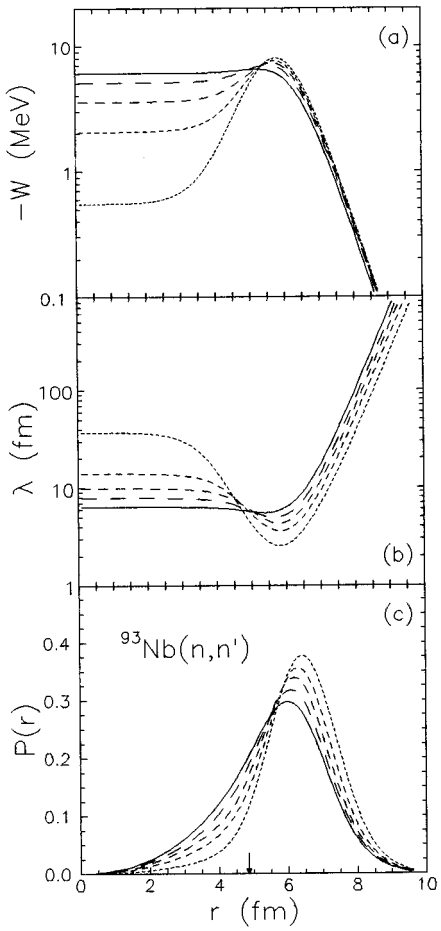

FIG. 1. Radial dependence of (a) the imaginary optical potential, (b) the corresponding local mean free path, and (c) the first *NN*-collision probability, for incident neutrons on ^{93}Nb with energies of 10 (dotted curves), 20 (short-dashed curves), 30 (dashed curves), 40 (long-dashed curves), and 50 MeV (solid curves). The OMP parameter set of Walter and Guss [37] is used. The arrow indicates the value of the half-density radius [44] of the nuclear matter density distribution for ^{93}Nb.

surface determines the MFP at low energies; i.e., there are smaller λ values than in the central nuclear region.

The first *NN*-collision probabilities corresponding to the imaginary potentials and $\lambda(r)$ values at different energies are shown in Fig. 1(c). Since the integral in Eq. (4) should be evaluated within the nuclear volume, the respective upper limit is chosen to be equal to the radius $R_s = r_D A^{1/3} + 6a_D$ at which the surface part of the imaginary potential is 1% of its central depth. A value of 0.1 fm has been used for the range $r - r'$, the results being insensitive to a smaller mesh size. The maximum of the $P(r)$ distribution within the nuclear surface, which becomes broader and moves slightly to smaller radii as the energy increases, is related mainly to the following points. First, it is due to the probability of the *NN* collision to occur at the radius r [see the second bracket in Eq. (10)]. It has a maximum at the surface and becomes rather constant inside the nuclear interior where the probability $P(r)$ for a given partial wave is still decreasing for lower r. The latter aspect is due to the fact that the incident particle has a constantly lower probability to penetrate the target nucleus further without any interaction. Actually this quantity entirely follows the maximum of the imaginary potential and the minimum of the MFP, respectively. Second, the averaging over the partial waves yields a small additional change of the maximum of $P(r)$ to larger radii and a significant decrease of its width especially for medium energies. This stronger surface character in comparison with the central collisions [36] is just related to the contributions of the peripheral trajectories.

The correctness of the present method to obtain and to take into account the surface character of the first *NN* collision by means of the radial dependence $P(r)$ can now be better estimated. The use of the quantal distorted waves makes it possible indeed to consider contributions from the regions which are innaccessible by the classical trajectories too. However, even the cross sections in the ''forbidden'' regions are still less significant [21] while the analysis of $P(r)$ suggests that such regions have lowest contribution to this quantity. This is also the meaning of the agreement found between the classical and quantal average flux and its divergence even for the neutron incident energies between 10 and 30 MeV [33] where a gradual transition to the pattern described by geometrical optics was noted (with the strongest change from 5 to 10 MeV). Keeping this in mind, in the next sections we analyze the average quantities which can be derived by using the first *NN*-collision probability $P(r)$.

III. AVERAGE FERMI ENERGY IN FIRST *NN* COLLISIONS

DeVries and DiGiacomo [30] showed that, due to the large variations of the local MFP, one must carefully identify the region in which the reaction takes place. Moreover, they found that it is necessary to look for a quantity which should include effects of the changing nuclear density and interactions along the path of the projectile. Actually, l-dependent average Fermi energies have been involved in the framework of the geometry-dependent hybrid (GDH) semiclassical model [15] to calculate the particle-hole state density in the first stage of the preequilibrium emission. While the Fermi energy at the saturation nuclear density ρ_0 is $E_F = 40$ MeV, a value around 30 MeV was found for $l=0$ and for higher partial waves it decreases as a function of the incident energy [17]. Kalbach [16] also took into account the surface effects for the first *NN* interaction by using a mean effective Fermi energy within the exciton model and found empirical values between 11 and 25 MeV in a broad target mass and incident energy range.

The local Fermi energy [25,39] (see also microscopical studies of the optical potential [19,38,40–42]) can be expressed within the local density approximation (LDA, e.g., [43]) in terms of the Fermi momentum and the nuclear density $\rho(r)$ as

$$E_F(r) = \frac{\hbar^2 k_F^2(\mathbf{r})}{2m} = \frac{\hbar^2}{2m}\left[\frac{3\pi^2}{2}\rho(\mathbf{r})\right]^{2/3}. \qquad (12)$$

Consequently, the Fermi energy averaged along the trajectory of the incident nucleon with respect to both the nuclear density and the first *NN*-collision probability becomes

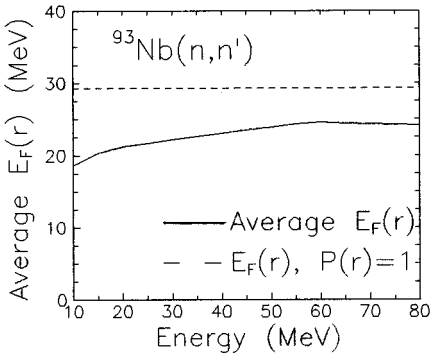

FIG. 2. Average local Fermi energy calculated for the first two-body collision in the case of ^{93}Nb(n,n') reaction (solid curve). The dashed curve corresponds to the assumption of an equiprobable site of interaction, i.e., to the use of the constant unity value for the first NN-collision probability $P(r)$.

$$\overline{E_F}=\frac{\int d\mathbf{r}\rho(\mathbf{r})P(r)E_F(r)}{\int d\mathbf{r}\rho(\mathbf{r})P(r)}=\frac{\int_0^{R_s}drr^2\rho(r)P(r)E_F(r)}{\int_0^{R_s}drr^2\rho(r)P(r)}. \tag{13}$$

The present formalism makes it possible to integrate over the whole nuclear volume without any additional assumption on the localization of the first NN collision [36].

The calculated average Fermi energy is shown in Fig. 2 for neutrons incident on ^{93}Nb in the energy range of the OMP parameter set of Walter and Guss [37]. The parametrization of Negele [44] has been used to describe the realistic nuclear matter distribution. As an independent test a separate calculation has been carried out by omitting the first NN-collision probability $P(r)$ in Eq. (13). This assumption of an equiprobable site of the interaction led to a constant average Fermi energy of $\sim$30 MeV (dashed line in Fig. 2). It reproduces the result of Blann for the complete s-wave penetration in the nucleus. At the same time, the comparison of the two average values of the Fermi energy illustrates the surface-localization effect for the first NN interaction in preequilibrium reactions. It is rather constant above the nucleon incident energy of 50 MeV (actually very slowly decreasing with energy) and stronger for lower energies. In fact, the physics comprised within the imaginary part of the optical potential is rejoined with respect to a quantity usually related to nuclear structure, in general agreement with the unified description of the mean field [38,40,41].

IV. AVERAGE STRENGTH OF THE EFFECTIVE INTERACTION

The recent systematic studies of the effective-interaction strength V_0 [3–7] and the sensitivity of the respective FKK calculations to the input parameters [3] pointed out the necessity to carry out such analyses by using the same standard parameter set over a wide range of the target mass number and incident energies. Various empirical values of V_0 from (n,n'), (p,xn), and (p,xp) reactions shown in Fig. 3 versus the incident energy satisfy this condition only in part. There is also an additional dependence of V_0 on the target-mass [45,46] and the neutron-proton distinguishability [3,4] which

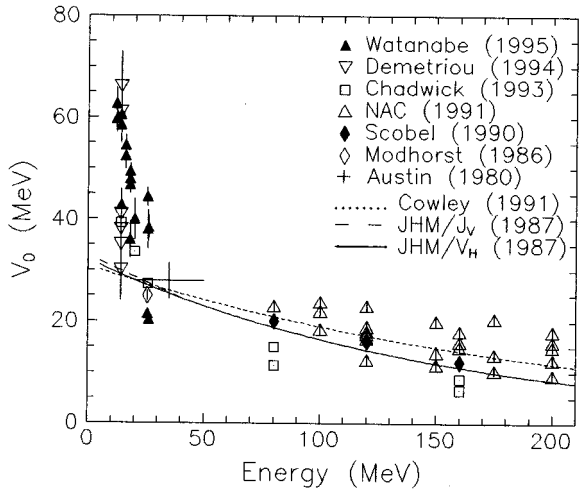

FIG. 3. Comparison of the effective NN-interaction strengths as functions of the incident energy obtained from FKK analyses of nucleon induced reactions using 1 fm range Yukawa form factor with the predictions of the normalized energy dependence of the nucleon optical potential obtained by Cowley *et al.* [48] (dotted curve), the Hartree-Fock component V_H of the real optical-potential depth (solid curve), and the volume integral per nucleon J_V/A of the full real potential (dashed curve) of Johnson *et al.* [41]. The points are from Watanabe *et al.* [3], Demetriou *et al.* [46], Chadwick *et al.* [23,52], NAC [45,48,53], Scobel *et al.* [54], Mordhorst *et al.* [55], and Austin [47].

increases the complexity of this figure. We will discuss in the following only the energy dependence of V_0.

The real part of the optical potential is given within the simple folding model approximation in terms of the nuclear density and the effective NN interaction (e.g., [47])

$$V(r)=\int d\mathbf{r}'\rho(\mathbf{r}')v_0(|\mathbf{r}-\mathbf{r}'|). \tag{14}$$

The relation between the respective volume integrals which follows from above,

$$\int d\mathbf{r}\, v_0(r)=\frac{1}{A}\int d\mathbf{r}\, V(r), \tag{15}$$

gives the strength of the 1 fm range Yukawa interaction $V_0=(1/4\pi)J_V/A$ as a function of the volume integral per nucleon of the real optical potential. It was argued [48] that the observed trend of the V_0 values should be consistent with the energy dependence of $V(r)$. The depth V_H of the Hartree-Fock component of the real optical potential found by Johnson *et al.* [41] for neutrons on lead in the energy domain [1,120 MeV] has been used in this respect [48] together with (i) a correction factor of $\frac{3}{4}$ for the gradual energy loss of the incident nucleon in the subsequent stages of the multistep process and (ii) a normalization at $E_i=20$ MeV to the V_0 value found in the DWBA analysis of (p,p') reaction at 20–50 MeV [47]. The form thus obtained,

$$V_0\simeq 30.8\exp(-0.15E_i/30.8), \tag{16}$$

is shown in Fig. 3. On the other hand, the above-mentioned relation between the effective interaction strength and the volume integral per nucleon of the same real optical potential [41] gives

$$V_0 = 0.727 V_H(E_i) = 33.7 \exp[-0.31(E_i - E_F)/46.4], \tag{17}$$

where E_F is the Fermi energy defined (opposite to the rest of this paper) with respect to the zero energy point. By adding the dispersive component to the Hartree-Fock one, Johnson *et al.* obtained also the volume integral for the full real potential [with the typical low-energy dependence implied by the use of the optical-potential dispersion relation (DR)] which yields similarly the form

$$V_0 = 32.8 - 0.207 E_i \quad \text{for } 4 < E_i < 40 \text{ MeV}, \tag{18}$$

which is shown in Fig. 3 in comparison with the prediction of Eq. (17). The correction factor for the gradual energy loss in the subsequent reaction steps should not be involved at low energies where the two-step scattering in the MSD process is negligibly small [23], so that the optical-model provisos seem to agree with the normalized energy dependence of Cowley *et al.* below, e.g., 50 MeV. However, the low-energy phenomenological V_0 values are much more increased in comparison with any predictions, including the additional dependence on the target-mass and the neutron-proton distinguishability. It is shown in the following that the nuclear-density dependence of the effective *NN* interaction may account for this, while other effects are avoided by considering only (n,n') and (p,p') reactions on ^{93}Nb.

First, Myers [49] described the density dependence of V_0 for a given incident energy by using a phenomenological factor which multiplies the effective *NN* interaction (see also [50])

$$f^E(\rho) = C_\rho(E_i)(1 - d\rho^{2/3}), \tag{19}$$

where $d = 2$ fm^2. Bonetti and Colombo [18] have already used this form within FKK calculations by taking the density-independent parameter $C_\rho = 1.4$ in order to obtain $f(\rho) = 1$ for $\rho = \frac{1}{3}\rho_0$. Next, Jeukenne *et al.* [51] showed that Eq. (14) becomes, in the frame of the LDA,

$$\frac{V(r)}{\rho(r)} = \int d\mathbf{r}' v_0(r'). \tag{20}$$

On the other hand, they found by means of the Brueckner-Hartree-Fock nuclear matter calculations that the contribution of the isoscalar component of the OMP to the left-hand side of Eq. (20) can be parametrized so that

$$\frac{V(r)}{\rho(r)} \approx F(E_i)[1 - d\rho^{2/3}(r)], \tag{21}$$

where $d = 2.03$ fm^2 and $F(E_i) = (903 - 7.67E_i + 0.022E_i^2)$ MeV fm^3, in the energy range [10,140 MeV]. By normalizing the factor $C_\rho(E_i)$ to this expression [50] we obtain a local density-dependent strength of the 1 fm range Yukawa interaction:

$$V_0(r, E_i) = \frac{1}{4\pi} F(E_i)[1 - d\rho^{2/3}(r)]. \tag{22}$$

In order to compare the results of this analysis with the phenomenological V_0 values we have to derive an average strength of the effective *NN* interaction along the trajectory of the incident nucleon. Therefore, we have obtained average $V_0(E_i)$ values for the first *NN* collision in multistep nuclear reactions by using a procedure similar to Eq. (13) for the average Fermi energy.

At the same time, the local density-dependent strength of the 1 fm range Yukawa interaction is given also by the left-hand side of Eq. (20) divided by 4π. Energy-dependent average V_0 values are calculated in this case but using now the real part of two optical potentials. The first one is that obtained by Johnson *et al.* [41] with the DR constraint, namely, the full potential for $E_i \leqslant 40$ MeV, and the Hartree-Fock component at higher energies where the respective volume integrals are similar. The second one is the global OMP of Walter and Guss [37], which was used in the systematic analysis of Watanabe *et al.* [3] and has been involved in this work to obtain the first *NN*-collision probability. The main reason to choose the latter OMP was the possibility to use neutron and proton optical potentials in which the asymmetry term has the same magnitude but opposite signs.

The average V_0 values for the first *NN* collision corresponding to both the local strengths of the effective *NN* interaction given by Eq. (22) and the use of the two OMP's are compared with the phenomenological V_0 values available from (n,n') and (p,p') reactions on ^{93}Nb in Fig. 4. The comparison is done in the energy range of the Walter-Guss OMP, being meaningful for low energies where the two-step contribution to the MSD process is negligibly small. The V_0 values predicted by the optical potential of Johnson *et al.* corresponding to Eq. (18) for $E_i \leqslant 40$ MeV and Eq. (17) at higher energies are shown in Fig. 4 as well. The effect of taking into account the density dependence of the effective *NN* interaction is obvious. This behavior is due to the well-known increase of the effective interaction as the nuclear density reduces [49] and to the increased surface localization of the first *NN* collision at lower energies (Fig. 1).

Before additional comments on the phenomenological and calculated effective *NN*-interaction strengths are made, we continue the interpretation of this quantity as a function of the local energy $E_i(\mathbf{r})$ introduced by Watanabe *et al.* [3]. The effects of the charge and isospin of the incident particle are properly taken into account when the local energy is estimated at realistic r values for a given projectile and incident energy. While Watanabe *et al.* considered the common nuclear radius $R = 1.25A^{1/3}$ fm in this respect, we take the advantage of having calculated the first *NN*-collision probability. Actually, we have derived an average value $E_i(r)$ of the local energy given by Eqs. (2) and (3) along the trajectory of the incident nucleon by using the same procedure of Eq. (13) as for the average Fermi energy E_F and the average effective *NN*-interaction strength V_0.

Finally, the phenomenological V_0 values of Watanabe *et al.* found from the analyses of the ^{93}Nb(n,n') and ^{98}Mo(p,p') reactions and the corresponding average V_0 values are shown in Fig. 5 versus the average local energy

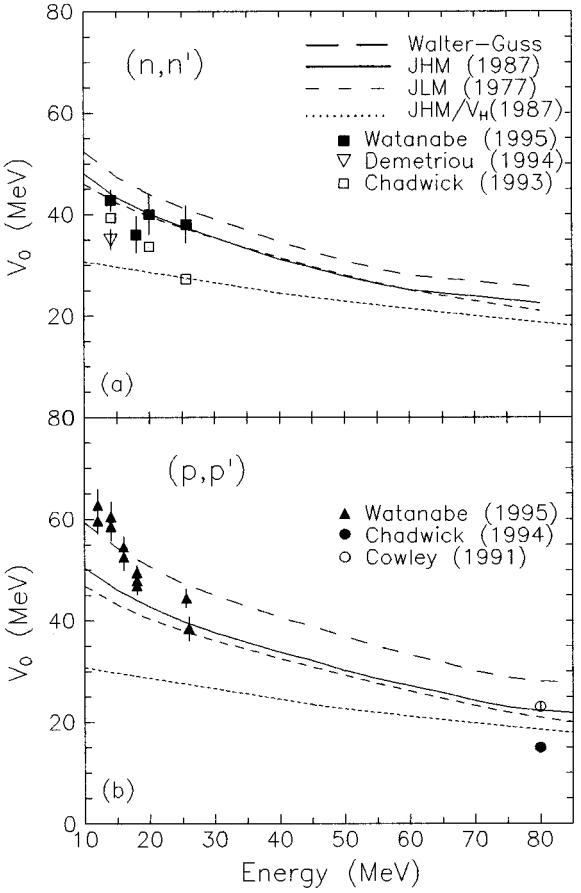

FIG. 4. The same as in Fig. 3 but for (a) (n,n') and (b) (p,p') reactions, and the V_0 predictions given by the optical potentials of Johnson *et al.* [41] (dotted curves), as well as the average local strengths obtained by using the same real potentials (solid curves), the OMP parameter set of Walter and Guss [37] (long-dashed curves), and the parametrization based on the Brueckner-Hartree-Fock nuclear matter calculations [51] (dashed curves). The points are from Watanabe *et al.* [3], Demetriou *et al.* [46], Chadwick *et al.* [23,52], and Cowley *et al.* [48].

$\overline{E_i}(r)$. First, the idea of using the local energy to understand the systematic trend of the strength V_0 is proved to go beyond the assumption that all two-body interactions occur just at the nuclear half-radius. Second, the use of quantities averaged by means of the first NN-collision probability over the nuclear volume seems to describe well the different strengths V_0 found by the studies of (n,n') and (p,p') reactions at the same low energy. This comment is justified especially when the OMP used to calculate the local effective NN-interaction strength includes a proper asymmetry term and works for both neutrons and protons. The rather lower V_0 values which correspond to the (n,n') reaction at a given average local energy $E_i(r)$ are predicted only by the Walter-Guss OMP (involved also in the analysis [3] which yields all V_0 data shown in Fig. 5). There is an opposite but small shift around 0.2–0.5 MeV between the other V_0 values calculated for the two reactions, only values for the (n,n') reaction being shown in the figure.

Coming back to the comparison given in Fig. 4, it can be seen that large differences between the various average V_0

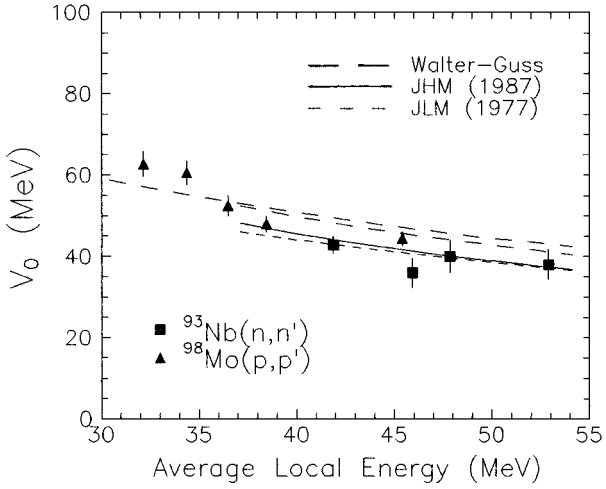

FIG. 5. The same as in Fig. 4 but for (n,n') and (p,p') reactions on ^{93}Nb, as a function of the average local energy for the first NN collision.

values correspond to the (p,p') reactions at lower energies [where the average local energy $E_i(r)$ is smallest too]. On the other hand, the agreement between the average strengths obtained with the Hartree-Fock potential plus the dispersive component [41] and by using the parametrization based on the Brueckner-Hartree-Fock nuclear matter calculations [51] is very good. The underestimation of the absolute V_0 values at the lowest incident energies by the latter approach originates from the similar behavior at small nuclear density of the expression $F(E_i)$ fitting the isoscalar real potential (Fig. 1 of [51]).

V. SUMMARY AND CONCLUSIONS

The objective of this work has been to study average quantities related to the characteristics of the NN interaction along the trajectory of the projectile in preequilibrium reactions. It is motivated first of all by the general use of semiclassical particle-hole state densities even at present within the FKK quantum formalism. This aspect could be connected with the discrepancies still existing in the systematics of the phenomenological effective NN-interaction strength V_0 values used in FKK-MSD calculations. At the same time, we have obtained similarly an average effective NN-interaction strength V_0 which is of interest for understanding of the V_0 systematics.

The basic element of our study has been the calculation of the radial dependence of the probability of the first two-body collision between the projectile and one of the target nucleons. It is carried out by using the semiclassical method to follow the incoming particle's path in the nuclear target. The particle curved trajectory as well as the momentum of the particle at each point of the trajectory, i.e., the NN-collision localization [20,21], can be considered providing the semiclassical approach is expected to be quantitatively reliable. The applicability of the semiclassical approximation below 50–100 MeV is yet an open question. However, there are evidences in this respect [31,33] while Kawai and co-workers [20–22] pointed out the limits in the

correctness of the respective results. The use of quantal distorted waves would make it possible to consider contributions from the regions which are innaccessible by the classical trajectories, while such regions have low contribution to the first NN-collision probability. Moreover, the shape we have obtained for the first NN-collision probability $P(r)$ as well as its use to derive average quantities of reaction models supports this approach.

The energy and radial dependences of the phenomenological imaginary part of the optical potential result in a minimum of $\lambda(r)$ in the region of the nuclear surface, taken into account earlier within the GDH model [15]. Next, we obtained a radial dependence $P(r)$ which evidences the surface character of the first NN collision. In the case of the GDH model Blann pointed out that only approximate averages of the imaginary potential and nuclear density over projectile trajectories for various partial waves have been used to determine the intranuclear transition rates, while *it has been assumed* that the reactions were localized within spherical shells determined by the projectile impact parameter.

The average Fermi energy in the first NN collision of preequilibrium reactions is then obtained by considering the local Fermi energy (expressed within the local density approximation) and averaging along the trajectory of the incident nucleon with respect to both the nuclear density and the first NN-collision probability. The present formalism allows one to integrate over the whole nuclear volume without any additional assumption on the localization of the first NN collision [36]. It should be noted that the assumption of an equiprobable site of interaction led to the constant average Fermi energy of $\sim$30 MeV [15]. The comparison of the two average values of the Fermi energy illustrates the effect of the surface localization of the first NN interaction, being stronger for energies lower than 50 MeV. We may refer again to the GDH model where the local Fermi energy value has been obtained within the LDA only from the density average along the projectile trajectory, as a first-order approximation intended to consider the geometry of the reaction with respect to the nuclear density distribution [15]. The present results confirm the geometry effect, while further comparison with the GDH conclusions will be obtained by inclusion of the actual average Fermi energy E_F in the particle-hole state density and reaction model formalism (a first attempt is made in Ref. [36]).

In order to compare the results of this analysis with the phenomenological V_0 values we have derived also an average strength of the effective NN interaction along the trajectory of the incident nucleon V_0 for the first NN collision in multistep reactions. Good agreement is found between the average strengths obtained with the Hartree-Fock potential plus the dispersive component [41] and by using the parametrization based on the Brueckner-Hartree-Fock nuclear matter calculations [51]. At the same time it turns out that the nuclear density dependence of the effective NN interaction may account for the low-energy phenomenological V_0 values which are much more increased in comparison with any predictions. Finally, the use of quantities averaged by means of the first NN-collision probability over the nuclear volume seems to describe well the different strengths V_0 found by the studies of (n,n') and (p,p') reactions at the same low energy [3]. These results support the application of the average Fermi energy within the particle-hole state densities used in the first stage of the multistep-reaction models.

ACKNOWLEDGMENTS

The authors are grateful to Professor M. Kawai for the careful reading of the manuscript and valuable discussions. This work was carried out under the Romanian Ministry of Research and Technology Contract No. 34/A12 and the Bulgarian National Science Foundation Contract No. Phi-406.

[1] E. Gadioli and P.E. Hodgson, *Pre-Equilibrium Nuclear Reactions* (Oxford University Press, Oxford, 1992).
[2] H. Feshbach, A. Kerman, and S. Koonin, Ann. Phys. (N.Y.) **125**, 429 (1980).
[3] Y. Watanabe, A. Aoto, H. Kashimoto, S. Chiba, T. Fukahori, K. Hasegawa, M. Mizumoto, S. Meigo, M. Sugimoto, Y. Yamanouti, N. Koori, M.B. Chadwick, and P.E. Hodgson, Phys. Rev. C **51**, 1891 (1995).
[4] Y. Watanabe, Acta Phys. Slovaca **45**, 749 (1995).
[5] W.A. Richter, Acta Phys. Slovaca **45**, 733 (1995).
[6] R. Lindsay, Acta Phys. Slovaca **45**, 717 (1995).
[7] P.E. Hodgson, Acta Phys. Slovaca **45**, 673 (1995).
[8] M. Herman, G. Reffo, H. Lenske, and H. Wolter, in *Proceedings of the International Conference on Nuclear Data for Science and Technology*, Gatlinburg, Tennessee, 1994, edited by J.K. Dickens (American Nuclear Society, La Grange Park, 1994), p. 466.
[9] K. Sato, Y. Takahashi, and S. Yoshida, Z. Phys. A **339**, 129 (1991).
[10] S. Yoshida, M. Abe, and K. Sato, Acta Phys. Slovaca **45**, 757 (1995).
[11] M. Blann and G. Reffo, in International Atomic Energy Agency Report No. INDC(NDS)-214/LJ, Vienna, 1989, p. 75.
[12] G. Reffo and M. Herman, in *Proceedings of the International Conference on Nuclear Data for Science and Technology*, Gatlinburg, Tennessee, 1994 [8], p. 473.
[13] F.C. Williams, Nucl. Phys. **A166**, 231 (1971).
[14] N. Austern, *Direct Nuclear Reaction Theories* (Wiley-Interscience, New York, 1970), p. 122.
[15] M. Blann, Phys. Rev. Let. **28**, 757 (1972); Nucl. Phys. **A213**, 570 (1973).
[16] C. Kalbach, Phys. Rev. C **32**, 1157 (1985).
[17] M. Avrigeanu and V. Avrigeanu, J. Phys. G **20**, 613 (1994).
[18] R. Bonetti and L. Colombo, Phys. Rev. C **28**, 980 (1983).
[19] M. Abe, S. Yoshida, and K. Sato, Phys. Rev. C **52**, 837 (1995).
[20] M. Kawai, Prog. Theor. Phys. **27**, 155 (1962).
[21] Y.L. Luo and M. Kawai, Phys. Rev. C **43**, 2367 (1991).
[22] M. Kawai and H.A. Weidenmüller, Phys. Rev. C **45**, 1856; Y. Watanabe and M. Kawai, Nucl. Phys. **A560**, 43 (1993); M. Kawai, Y. Watanabe, and H. Shinohara, Acta Phys. Slovaca **45**, 693 (1995).

[23] M.B. Chadwick and P.G. Young, Phys. Rev. C **47**, 2255 (1993).
[24] A. Nadasen, P. Schwandt, P.P. Singh, W.W. Jacobs, A.D. Bacher, P.T. Debevec, M.D. Kaitchuck, and J.T. Meek, Phys. Rev. C **23**, 1023 (1981).
[25] K. Kikuchi and M. Kawai, *Nuclear Matter and Nuclear Reactions* (North-Holland, Amsterdam, 1968).
[26] J.W. Negele and K. Yazaki, Phys. Rev. Lett. **47**, 71 (1981).
[27] V.R. Pandharipande and S.C. Pieper, Phys. Rev. C **45**, 791 (1992).
[28] R. Crespo, R.C. Johnson, J.A. Tostevin, R.S. Mackintosh, and S.G. Cooper, Phys. Rev. C **49**, 1091 (1994).
[29] H.O. Meyer and P. Schwandt, Phys. Lett. **107B**, 353 (1981).
[30] R.M. DeVries and N.J. DiGiacomo, J. Phys. G **7**, L51 (1981).
[31] H.C. Chiang and J. Hüfner, Nucl. Phys. **A349**, 466 (1980).
[32] H. Feshbach, *Theoretical Nuclear Physics* (Wiley, New York, 1992), p. 409.
[33] I.E. McCarthy, Nucl. Phys. **11**, 574 (1959); **10**, 583 (1959).
[34] W.Q. Chao, F. Hachenberg, and J. Hüfner, Nucl. Phys. **A384**, 24 (1982).
[35] R.O. Newton, *Scattering Theory of Waves and Particles* (McGraw-Hill, New York, 1966), p. 583.
[36] M. Avrigeanu, A. Harangozo, V. Avrigeanu, and A. N. Antonov, Acta Phys. Slovaca **45**, 617 (1995).
[37] R.L. Walter and P.P. Guss, Radiat. Eff. **95**, 73 (1986).
[38] R.W. Hasse and P. Schuck, Nucl. Phys. **A445** 205 (1985).
[39] K. Chen, Z. Fraenkel, G. Friedlander, J.R. Grover, J.M. Miller, and Y. Shimamoto, Phys. Rev. **166**, 949 (1968).
[40] R.W. Hasse and P. Schuck, Nucl. Phys. **A438** 157 (1985).
[41] C. H. Johnson, D. J. Horen, and C. Mahaux, Phys. Rev. C **36**, 2252 (1987).
[42] K. Sato and S. Yoshida, Phys. Rev. C **49**, 1099 (1994).
[43] A.N. Antonov, P.E. Hodgson, and I.Zh. Petkov, *Nucleon Momentum and Density Distributions in Nuclei* (Clarendon Press, Oxford, 1988), p. 22.
[44] J.W. Negele, Phys. Rev. C **1**, 1260 (1970).
[45] W.A. Richter, A.A. Cowley, R. Lindsay, J.J. Lawrie, S.V. Fortsch, J.V. Pilcher, R. Bonetti, and P.E. Hodgson, Phys. Rev. C **46**, 1030 (1992).
[46] P. Demetriou, P. Kanjanarat, and P.E. Hodgson, J. Phys. G **19**, L193 (1993); **20**, 1779 (1994).
[47] S. M. Austin, in *The (p,n) Reaction and the Nucleon-Nucleon Force*, edited by C. D. Goodman *et al.* (Plenum, New York,1980), p. 203.
[48] A.A. Cowley, A. van Kent, J.J. Lawrie, S.V. Fortsch, D.M. Whittal, J.V. Pilcher, F.D. Smit, W.A. Richter, R. Lindsay, I.J. van Heerden, R. Bonetti, and P.E. Hodgson, Phys. Rev. C **43**, 678 (1991).
[49] W.D. Myers, Nucl. Phys. **A204**, 465 (1973).
[50] A.M. Kobos, B.A. Brown, P.E. Hodgson, G.R. Satchler, and A. Budzanowski, Nucl. Phys. **A384**, 65 (1982).
[51] J.-P. Jeukenne, A. Lejeune, and C. Mahaux, Phys. Rev. C **16**, 80 (1977).
[52] M.B. Chadwick, P.G. Young, D.C. George, and Y. Watanabe, Phys. Rev. C **50**, 966 (1994).
[53] W.A. Richter, A.A. Cowley, G.C. Hillhouse, J.A. Stander, J.W. Kohen, S.W. Steyn, R. Lindsay, R.E. Julies, J.J. Lawrie, J.V. Pilcher, and P.E. Hodgson, Phys. Rev. C **49**, 1001 (1994).
[54] W. Scobel, M. Trabandt, M. Blann, B.A. Pohl, B.R. Remington, R.C. Byrd, C.C. Foster, R. Bonetti, C. Chiesa, and S.M. Grimes, Phys. Rev. C **41**, 2010 (1990).
[55] E. Mordhorst, M. Trabandt, A. Kaminsky, H. Krause, W. Scobel, R. Bonetti, and F. Crespi, Phys. Rev. C **34**, 103 (1986).